Chapter 3
Thermal Properties

Mateusz Wyrzykowski, Agnieszka Knoppik, Wilson R. Leal da Silva, Pietro Lura, Tulio Honorio, Yunus Ballim, Brice Delsaute, Stéphanie Staquet and Miguel Azenha

Abstract This chapter is dedicated to relevant thermal properties in the scope of massive concrete structures. The initial part of the chapter (Sect. 3.1) pertains to properties that affect internal temperature developments in concrete, namely the thermal conductivity, the heat capacity and the heat exchanges between concrete and the surrounding media. The final part of the chapter (Sect. 3.2) is devoted to the thermal expansion coefficient, which is of fundamental importance to understand and predict the actual volume changes that take place in massive structures due to temperature variations.

M. Wyrzykowski (✉) · P. Lura
Empa, Swiss Federal Laboratories for Materials Science and Technology,
Dübendorf, Switzerland
e-mail: mateusz.wyrzykowski@empa.ch

A. Knoppik
Silesian University of Technology, Gliwice, Poland

W. R. Leal da Silva
Danish Technological Institute, Gregersensvej 4, 2630 Taastrup, Denmark

P. Lura
Institute for Building Materials, ETH Zurich, Zürich, Switzerland

T. Honorio
Laboratoire d'Etude du Comportement des Bétons et des Argiles, CEA, DEN,
DPC, SECR, 91191 Gif-sur-Yvette, France

Y. Ballim
University of the Witwatersrand, Johannesburg, South Africa

B. Delsaute · S. Staquet
BATir, LGC, Université Libre de Bruxelles, Brussels, Belgium

M. Azenha
ISISE, University of Minho, Guimarães, Portugal

E. M. R. Fairbairn and M. Azenha (eds.), *Thermal Cracking of Massive Concrete Structures*, RILEM State-of-the-Art Reports 27,
https://doi.org/10.1007/978-3-319-76617-1_3

3.1 Heat Transport and Temperature Change

In this section, properties governing the transfer of heat and the corresponding changes of temperature in concrete are discussed. In order to analyse these properties, a brief discussion of the mechanisms of heat transport is necessary, together with a commonly applied description of heat transport. Temperature evolution and heat transport in hydrating concrete can be described at the macroscale level by means of the following equation, e.g. Coussy (2005); Ulm and Coussy (2001); Klemczak (2011); Gawin et al. (2006); Azenha et al. (2011):

$$\rho C_p \frac{\partial T}{\partial t} = div(\lambda_{eff}\, grad\, T) + \frac{\partial Q}{\partial t} \tag{3.1}$$

where ρ is the concrete density, C_p is the specific heat capacity (ρC_p is the volumetric heat capacity), T is the temperature, t is the time, λ_{eff} is the effective thermal conductivity and Q is the volumetric heat produced due to hydration of binder (see Chap. 2). C_p, ρ and λ_{eff} are dependent on degree of hydration, moisture content and temperature. In some cases, due to anisotropy of the material, λ_{eff} may be expressed as a tensor instead of a scalar (Eq. (3.1) remains valid in this case). The boundary conditions for Eq. 3.1 are described in Sect. 3.1.3, while the initial conditions refer to fresh concrete temperature corresponding to the start of the analysis.

After simple transformations of Eq. 3.1, the temperature change in time is described with the following equation:

$$\frac{\partial T}{\partial t} = \frac{1}{\rho C_p} div(\lambda_{eff}\, grad\, T) + \frac{\partial \alpha}{\partial t}\frac{Q_\infty}{\rho C_p} \tag{3.2}$$

where α is the degree of hydration (see Chap. 2) and Q_∞ is the total volumetric heat of hydration, with $\partial Q/\partial t = \partial \alpha/\partial t \cdot Q_\infty$ (see Eq. 3.2). The last term in Eq. 3.2 represents the adiabatic temperature rise in concrete, and it is often used as a reasonable and safe estimation of the maximum temperature rise that might be expected in a massive structure, as shown, e.g., by Ulm and Coussy (2001). After assuming that the thermal conductivity does not depend on temperature for the temperatures normally encountered in massive structures (see Sect. 3.1.1) (Gawin et al. 1999), the problem becomes linear, and the term $\lambda_{eff}/(\rho C_p)$ can be conveniently used as thermal diffusion coefficient, e.g. Klemczak (2011); Ulm and Coussy (2001).

Equation 3.2 demonstrates that the most basic description of temperature changes due to heat transfer in concrete requires two parameters: effective heat conductivity and heat capacity. It needs to be mentioned here that such description is necessarily simplified since it does not take into account the heat transport related to migration of water in early-age concrete. In this case, migration of water in the pores towards the drying surfaces (or, from the wetted surfaces to the self-desiccated bulk) and the possible phase changes of water will cause associated heat transport. In order to describe this process, the heat transport equation needs to be coupled with an appropriate mass balance equation of water, e.g. Gawin et al. (2006); Azenha et al. (2011). Optionally, an additional transport term may be added to Eq. 3.1 or Eq. 3.2 due to water transport, with a thermohygral thermal diffusion coefficient, see, e.g., Klemczak (2011). It can be expected that the thermohygral heat transport is more important for the surface temperature (in particular at the removal of formworks and evaporative cooling) than for the temperature evolution in the bulk (McCarter and Ben-Saleh 2001). Kovler (1995) reported about an experimental programme on the shock of evaporative cooling of concrete in hot dry climate. The importance of evaporative cooling in thin specimens was later confirmed in experiments and simulations by Azenha (2009).

The thermal properties of concrete depend strongly on the thermal properties of its components. Initially, this is reflected as a dependence upon mix composition. Further, hardening of concrete is related to, and accompanied by, various phenomena of chemo-physical nature that are due to the ongoing reaction of the cement and to interactions of the concrete with the environment. These processes cause an evolution of thermal properties of mainly the cement paste, and as a consequence, of the concrete (as evidenced, e.g., based on measurements of thermal expansion coefficient in Wyrzykowski and Lura (2013a). The thermal properties of concrete change during hardening due to (a) changes of moisture state (water content in pores) resulting from hydration (as water is consumed in the reaction) and interaction with the environment (drying/wetting), and (b) degree of hydration since cement hydration leads also to changes in volumes of unhydrated cement, hydrates and porosity in addition to changes of moisture state. As it will be shown later in the chapter, the first-order effect is due to changes of moisture state, while hydration can be in many cases neglected.

3.1.1 Thermal Conductivity

Effective thermal conductivity of concrete, λ_{eff}, describes the ability of concrete to conduct heat at the macroscopic level. In Eq. 3.1, heat flux is conveniently described at the macroscopic level as heat conduction with Fourier's law, whereby heat fluxes, q, perpendicular to a given surface (with unit area) can be described by: $q = -\lambda_{eff}\, gradT$. It needs to be noted that such description corresponds in fact to an effective conductivity that accounts for the coupled effect of different heat transfer mechanisms occurring at the microstructural scale due to convection and radiation in the desaturated pores in addition to conduction within different concrete components (i.e. hydration products, aggregates, cement, water) (Litovsky and Shapiro 1992).

Thermal conductivity can be determined for concrete using a variety of methods that are generally based on the principle of generating a temperature gradient in a sample and measuring the corresponding temperature distribution either after establishing equilibrium conditions and a constant temperature gradient (steady-state methods) or in a relatively short time during or following heating (transient methods). Depending on the technique, the temperature gradient can be obtained by heating the sample at one point and/or cooling the sample at a distant point, while measuring the temperature at a given point of the sample or directly on the heating/cooling element (Campbell-Allen and Thorne 1963; Mounanga et al. 2004). One of the commonly used standard methods based on heating and measuring the temperature at the same point in a sample is the so-called transient hot wire method (ASTM 1113), where a wire is placed in the sample and heated by means of electrical current. The wire works as a resistive thermometer at the same time—the rate at which the temperature of the wire increases can be then correlated with the heat transfer (heat conductivity) within the sample. Other commonly used methods are based on placing a planar sample between a heated and a cooled plate (e.g. the so-called guarded hot plate method) (Hammerschmidt 2002) or placing a heater and a thermometer in distant holes in the sample (e.g. two-linear-parallel-probe method) (Morabito 1989).

The most relevant factors affecting thermal conductivity of concrete are aggregate volume fraction, air content and moisture state of concrete, e.g. Kim et al. (2003). Furthermore, it was also found that the age itself has a negligible net effect on the thermal conductivity of concrete, except for very early ages, i.e. below about 2 days (Kim et al. 2003, Bentz 2008, Gibbon and Ballim 1998). According to Bentz (2008) this is because the thermal conductivity of cement paste components (water: 0.604 W/(mK) and cement: 1.55 W/(mK)) and hydrated cement paste are close enough so that the percolation of solids or depercolation of porosity can have only a limited impact on this property (about ±10%). The thermal conductivity of the main hydration products, i.e. C–S–H and CH, has been reported as 0.978 W/(mK) and 1.32 W(mK), respectively (Abdolhosseini Qomi et al. 2015), see also Table 3.1. The thermal conductivity of cement paste is consequently around 1.0 W/(mK). From this point of view, admixtures can have only negligible effect on the thermal conductivity.

Moist concrete has higher thermal conductivity than dry concrete since water contained in pores is more conductive than air. Consequently, ordinary concretes have conductivity about 1.0 W/(mK) higher in moist condition compared to dry condition (Tatro 2006), see Table 3.2. Guo et al. (2011) determined thermal conductivity of concrete mixtures at 20 °C with aggregate volume ratio of 70% as equal to 1.96 and 2.47 W/(mK) for dry conditions and wet conditions, respectively.

With increasing air content, the thermal conductivity of concrete decreases. This is especially pronounced for insulating concrete, where high air content is obtained by means of aerating or using lightweight aggregates. Values below 0.3 W/(mK) for aerated concrete were reported in Tatro (2006).

A comprehensive list of thermal conductivity values for concrete mixtures produced with different types of aggregates measured at various temperatures is available in ACI 207.1 (2005). The presented values range from 1.84 to 3.70 W/(mK).

Table 3.1 Thermal properties: results for temperatures ranging from 10 to 30 °C (adapted from Honorio 2015; Honorio et al. 2018)

Compound		Specific heat [J/(gK)]	Thermal conductivity [W/(mK)]
(Free) Water		4.183 (Holman 2009)	0.608 (Vargaftik 1993)
Clinker, clinker phases, gypsum	Clinker	0.750 (Bentz 2007)	1.55 (Bentz 2007)
	C_3S	0.745 (Lothenbach et al. 2008) 0.710 (Abdolhosseini Qomi et al. 2015)[a] 0.710 (Matschei et al. 2007) 0.750 (Todd 1951)	3.35 (Abdolhosseini Qomi et al. 2015)[a]
	C_2S	0.741 (Lothenbach et al. 2008) 0.720 (Abdolhosseini Qomi et al. 2015)[a] 0.720 (Matschei et al. 2007) 0.750 (Todd 1951)	3.45 (Abdolhosseini Qomi et al. 2015)[a]
	C_3A	0.768 (Lothenbach et al. 2008)	–
	C_4AF	0.813 (Lothenbach et al. 2008) 20 °C	–
	Gypsum	1.080 (Bentz and Prasad 2007)	0.66 (Cerny and Rovnanikova 2002) 1.26 (Côté and Konrad 2005)
Hydration products	C–S–H	0.950 (Cerny and Rovnanikova 2002) 722 (Lothenbach et al. 2008)	0.978 (Abdolhosseini Qomi et al. 2015)[a]
	CH	1.140 (Abdolhosseini Qomi et al. 2015)[a] 1.150 (Matschei et al. 2007)	1.32 (Abdolhosseini Qomi et al. 2015)[a]
	AFt	1.502 (Lothenbach et al. 2008)	–
	AFm	0.888–1.115 (Baquerizo et al. 2015)	–
	Hydrogarnet	0.666–1.121 (Matschei et al. 2007)	–
Cement-based composite materials	Cement paste	1.100–1.800 (Bentz 2007)	0.53–1.16 (Bentz 2007)
	Mortar	0.642 (Xu and Chung 2000)	0.9–1.5 (Cerny and Rovnanikova 2002) 1.37–2.65 (Khan 2002)
	Concrete	1.109–1.590	1.2–2.0 (Cerny and Rovnanikova 2002) 1.60–4.18 (Khan 2002)

(continued)

Table 3.1 (continued)

Compound		Specific heat [J/(gK)]	Thermal conductivity [W/(mK)]
Aggregates	Limestone aggregates	0.845 (Marshall 1972)	3.15–3.23 (Cerny and Rovnanikova 2002) 3.22 (Marshall 1972) 2.65–3.22 (Kim et al. 2003)
	Siliceous aggregates	–	2.90–5.18 (Cerny and Rovnanikova 2002) 5.16 (Kim et al. 2003)
	Basalt	0.766 (Marshall 1972)	4.03–4.30 (Khan 2002) 2.86 (Kim et al. 2003) 1.70 (Marshall 1972)

[a] Molecular simulations

Table 3.2 Effect of different aggregates and moisture conditions on thermal conductivity of concrete (Tatro 2006)

Aggregate type	Thermal conductivity —wet state [W/mK]	Thermal conductivity —50% RH [W/mK]	Thermal conductivity —dry state [W/mK]
Limestone	2.2	1.7	1.4
Sandstone	2.9	2.2	1.4
Quartz	3.3	2.7	2.3
Basalt	1.9–2.0	–	1.7
Expanded shale	0.85	0.79	0.62

Considering that the conductivity of concrete depends strongly on the type and amount of aggregates, and it is further affected by the air content, it can be considered as dependent on the concrete density.

Although the unit mass and moisture conditions of concrete, which are considered a key factor affecting conductivity (Neville 1997; Mehta and Monteiro 2005), are not reported in ACI 207.1 (2005), the range of values is also within the limits presented in Neville (1997). Another comprehensive list is presented in Tatro (2006).

Table 3.1 summarizes thermal conductivities of concrete components and exemplary concretes, while Table 3.2 summarizes the effect of aggregate types and moisture conditions on thermal conductivity.

Different authors proposed numerous analytical approaches for simulating the development of the thermal conductivity. The simplest approach consists of lumping the overall effect of concrete microstructure development and pores desaturation and describing the temperature evolution as a linear function of degree of hydration, e.g., Reinhardt et al. (1982); de Borst and van den Boogaard (1994); Ruiz et al. (2001):

$$\lambda_{eff} = \lambda_0(a_1 - a_2 \cdot \alpha(t)) \tag{3.3}$$

where λ_0 represents the final value of thermal conductivity and a_1, a_2 are empirical constants. For example, Ruiz et al. 2001 proposed $a_1 = 1.33$ and $a_2 = 0.33$. It needs to be noted, however, that many authors obtained good numerical predictions by neglecting the change of the values of thermal conductivity and using average values based only on mix composition (de Schutter 2002; Faria et al. 2006; Craeye et al. 2009; Zreiki et al. 2010; Briffaut et al. 2012). It was shown by Azenha (2009) and Briffaut et al. (2012) that the assumption of constant values of thermal parameters of concrete yields conservative predictions (expected temperatures are overestimated).

More complex approaches allow to account for different effects influencing the development of thermal conductivity. An empirical equation obtained based on a comprehensive experimental study developed by Kim et al. (2003) reads:

$$\begin{aligned}\lambda_{eff} = \lambda_{ref}(0.293 + 1.01A_R)(0.2RH + 0.8(1.62 - 1.54w/c))\\ \times\ (1.05 - 0.0025T)(0.86 + 0.0036F_R)\end{aligned} \tag{3.4}$$

where A_R and F_R correspond to the total and fine aggregate volumetric ratios, respectively, w/c is the water-to-cement ratio, RH is the relative humidity and λ_{ref} is the reference value of thermal conductivity. The latter is obtained from experimental measurements of reference concrete with $A_R = 0.70$, $w/c = 0.40$, $T = 20$ °C and $RH = 100\%$.

Another approach to account for the moisture content has been applied by Gawin et al. (2006):

$$\lambda_{eff} = \lambda_{dry}\left(1 + \frac{4 \cdot \Phi \cdot \rho_w \cdot S_w}{(1 - \Phi)\rho_s}\right) \tag{3.5}$$

where λ_{dry} is thermal conductivity of dry concrete, Φ is porosity (incorporating the effect of changes due to ongoing hydration), ρ_w and ρ_s are the densities of water and solid skeleton (dry concrete), respectively, and S_w is the saturation degree of pores with water.

The thermal conductivity of concrete based on its composition can be predicted using Mori-Tanaka scheme (Bohm and Nogales 2008) by homogenizing the thermal conductivities of the components: cement paste and aggregates, assuming the latter all have the same thermal conductivity:

$$\lambda_{eff} = \lambda_{paste} + \frac{3f_{agg}\lambda_{paste}(\lambda_{agg} - \lambda_{paste})}{3\lambda_{paste} + f_{paste}(\lambda_{agg} - \lambda_{paste})} \tag{3.6}$$

where f is the volumetric fraction. In particular, the Mori-Tanaka scheme in this form assumes concrete as a macro-isotropic composite material that is composed of a continuous morphologically prevailing matrix (cement paste) and reinforced by isotropic spherical inclusions distributed homogeneously in the matrix. These inclusions correspond to, e.g., aggregates. It should be considered that the defects, e.g. microcracks or regions of increased porosity, are not accounted for; they may play an important role in the thermal conductivity of solids (e.g. Litovsky and Shapiro (1992); Honorio et al. (2018)). Moreover, specific transfer effects in pores (namely, fluid conductivity, thermal radiation, convection and surface heterogeneous phenomena (Litovsky and Shapiro 1992)) are in general neglected in multiscale estimation of thermal conductivity.

A further, simpler approximation can be obtained by mass averaging of thermal conductivities of concrete components (Zreiki et al. 2010; Jendele et al. 2014):

$$\lambda_{eff} = \sum\nolimits_i m_i \cdot \lambda_i \tag{3.7}$$

where m_i is the weight ratio of subsequent components. Such formulation is only a very rough approximation, since it assumes that the constituents are arranged in parallel.

Thermal conductivities of concrete mix components are listed in Table 3.1.

Gawin et al. (1999) stated that the dependence of the thermal conductivity upon temperature can be neglected for the temperature ranges encountered in hardening concrete. For example, an empirical relation used by Gawin et al. (1999) for their simulations of concrete at fire assumes a change of λ of +0.0005 W/(mK) per +1 K of temperature change. The effect of temperature in the range 21–54 °C on the thermal conductivity was also neglected by van Breugel (1980).

In simulations of concrete structures, Briffaut et al. (2012) observed that the computed stresses were only slightly affected by temperature and age dependence of thermal conductivity.

3.1.2 Heat Capacity

Specific heat capacity C_p is the amount of energy in [J], necessary to raise 1 unit mass, [g], of a given material by a unit of temperature, [K].

Experimental measurements of heat capacity in concrete involve the same principle as the measurements of thermal conductivity, see Sect. 3.1.1, with dynamic thermal (transient) measurements, e.g. Pomianowski et al. (2014), or a combination of transient and steady-state measurements, where the heat capacity is calculated based on the thermal diffusion coefficient (obtained from the transient method) and the heat conductivity (obtained from the steady-state method), e.g. Luca and Mrawira (2005).

Similarly to thermal conductivity, the heat capacity of concrete depends strongly on thermal capacities of the different components i. Its value can be estimated through the rule of mixtures (Bentz 2007) based on mass fractions of the components, m_i, as long as the specific heat capacity of each independent phase, C_i, is known. This way, the specific heat capacity of concrete is computed as follows:

$$C_p = \sum_i m_i \cdot C_i \tag{3.8}$$

The heat capacity of the aggregates depends on their mineralogical characteristics. Reference values of specific heat capacity for different aggregates are reported in Choktaweekarn and Tangtermsirikul (2010), Hamzah et al. (2010), Honorio (2015) and collected in Table 3.1.

The evolution of heat capacity during hardening is driven, similarly to the thermal conductivity, mainly by changes in water content and microstructural evolution due to hydration. The specific heat capacity of cement powder is typically equal to about 0.75 J/(gK) (Bentz 2008; Bentz et al. 2011), while the specific heat capacity of water is equal to 4.18 J/(gK). Nonetheless, as water becomes incorporated into hydration products, its effective heat capacity is considerably reduced to 2.20 J/(gK), as suggested by (Bentz 2007). Molecular simulations confirm that the heat capacity of confined water in C–S–H is reduced with respect to bulk (or free) water (Abdolhosseini Qomi et al. 2015). Since volume (or mass) and energy are extensive thermodynamic quantities, upscaling heat capacity can be done by the rule of mixtures (assuming that surface effects are negligible). As shown by Bentz (2007, 2008), the heat capacity of cement paste can be also approximated as a function of its degree of hydration α. In particular, Eq. 3.9 is suggested to compute the evolution of heat capacity in sealed conditions (Bentz 2007):

$$C_p(\alpha) = C_p(\alpha_0) \cdot [1.0 - 0.26 \cdot (1 - e^{-2.9\alpha})] \tag{3.9}$$

where $C_p(\alpha_0) = C_w(\alpha_0) \cdot m_w(\alpha_0) + C_c(\alpha_0) \cdot m_c(\alpha_0)$ is the heat capacity of cement paste at initial degree of hydration α_0, calculated as a weighted average (with m being mass fractions of constituents w and c). The subscripts w and c correspond to water and cement. Based on the C_w and C_c values recommended by Bentz et al. (2011), C_p at α_0 reads:

$$C_p(\alpha_0) = 4.18 m_w(\alpha_0) + 0.75(\alpha_0) \tag{3.10}$$

As an example, Eqs. 3.8–3.10 were used by Lura and van Breugel (2001) to estimate values of concrete heat capacity for concrete mixtures containing 47% of granite and 34% of quartz sand by mass of dry materials. The heat capacity of sand and coarse aggregates was set at 0.80 and 0.61 J/(gK) (Choktaweekarn and Tangtermsirikul 2010; Hamzah et al. 2010). The results from this example are shown in Fig. 3.1.

The values in Fig. 3.1 are within the common range of heat capacity for ordinary concrete, i.e. from 0.84 to 1.17 J/(gK) (Neville 1997). The variable aspect of heat capacity is reported to impact significantly the mechanical response of concrete structures at early age. Lura and van Breugel (2001) found that a given percentage

Fig. 3.1 Heat capacity for cement paste and concrete predicted by the rule of mixtures (C_{fg} = 0.80 J/(gK), C_{cg} = 0.61 J/(gK), C_c = 0.75 J/(gK), and C_w = 4.18 J/(gK))

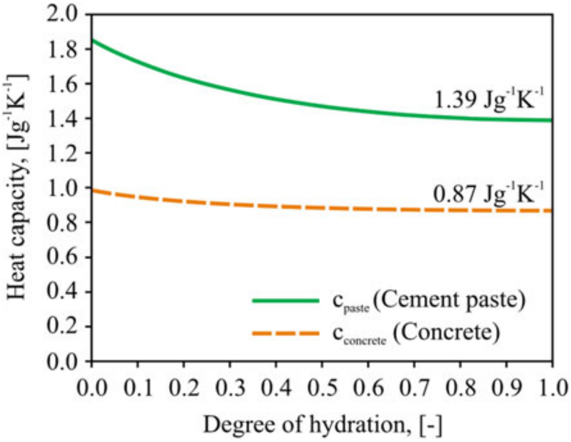

of variation of the heat capacity may lead to a percentage of variation in the same order of magnitude in the computed stresses. Briffaut et al. (2012), in simulations with varying heat capacity, found stresses roughly 20% inferior to the stresses computed in a scenario with constant heat capacity.

The specific heat increases with temperature. In Tatro (2006), specific heat values of 0.92 and 1.04 J/(gK) were reported for temperatures of 10 °C and 66 °C, respectively.

3.1.3 Exchange of Heat with the Environment

Heat transport in concrete and the resulting temperature evolution are affected by heat exchange with the environment at the boundaries. For describing this process, boundary conditions of the III type (a linear combination of the value of a variable, i.e. temperature, and of its derivative at the boundary, i.e. heat transfer coefficient) are usually applied, e.g. Gawin et al. (2006). A heat transfer coefficient (also referred to as the heat exchange coefficient) is in general dependent upon both the characteristics of the concrete surface and the environment. Comprehensive studies on heat exchange of concrete with the environment have been presented, e.g., in Jonasson (1994) or Wojcik (2001); Wojcik et al. (2003).

Heat exchange at the open boundaries of concrete can take place due to thermal radiation and convection (Kusuda 1977). Thermal radiation occurs as energy is emitted in the form of electromagnetic waves. In convection, heat is exchanged due to movement (natural or forced) of fluids, in this case, of air in contact with the concrete surface. The heat exchange due to convection is approximately proportional to the temperature difference ($T - T_\infty$) between the concrete surface T and the surroundings T_∞ according to Newton's law of cooling, while heat exchange due to radiation is proportional to differences of temperatures in absolute scale to the power of four, i.e. ($T^4 - T_\infty^4$) according to the Stefan–Boltzmann law (Modest 2013).

Usually, the two phenomena are considered together by means of one coefficient that accounts for both convection, h_p, and radiation, h_r (Faria et al. 2006):

$$h_{pr} = h_p + h_r \tag{3.11}$$

The coefficient of heat exchange by radiation, h_r, can be approximated by simplifying the 4th power radiative heat exchange law, for a given ambient temperature, $\mathrm{T_a} > 5$ °C, and the emissivity of concrete, *e*, as follows (Branco et al. 1992):

$$h_r = \mathrm{e}[4.8 + 0.075(T_a - 5)] \tag{3.12}$$

In addition to radiative heating of concrete surfaces by the sun, radiative heat exchange can be especially important for mass concrete with regard to the night cooling effect, leading to significant daily temperature amplitudes. As estimated by Michell and Biggs (1979), a black body exposed to the clear sky at night may be cooled even 10–12 °C below ambient temperature. No indications for concrete are known, but a similar temperature difference of 10 °C has been measured for metal roof on a clear night by Hollick (2012).

The convective heat exchange coefficient at the concrete surface is influenced by geometric and aerodynamic parameters (Kim et al. 2003; Bentz 2008; Lee et al. 2009). The coefficient of heat exchange by free convection for concrete can be assumed as equal to h_p = 6.0 W/(m^{2}K) in stagnant air conditions (Branco et al. 1992). The heat exchange coefficient varies with the wind speed (Kwak et al. 2006; Briffaut et al. 2012). To account for forced convection due to wind action, the heat exchange coefficient is defined as a function of wind speed, v [m/s], according to different authors as follows:

- Branco et al. (1992):

$$h_p = 3.7v \tag{3.13}$$

- Jonasson (1994):

$$h_p = 5.6 + 3.95v \quad \text{if } v < 5\frac{m}{s}$$

$$h_p = 7.6v^{0.78} \text{ if } v > 5\frac{m}{s} \tag{3.14}$$

- Briffaut et al. (2012), as a function of the wind speed, dimensions of the structure, ambient temperature:

$$\begin{aligned} h_p &= 0.13\left(\frac{g\,\alpha_{T,flu} l_{c,Cr}}{\upsilon_f D_t}(T_1 - T_a)\right)^{1/3}\left(\frac{\lambda_{flu}}{l_{c,Cr}}\right) && \text{for natural convection} \\ h_p &= 0.664\left(\frac{v\,l_{c,\mathrm{Re}}}{\upsilon_f}\right)^{1/2}\left(\frac{\upsilon_f}{D_t}\right)^{1/3}\left(\frac{\lambda_{flu}}{l_{c,\mathrm{Re}}}\right) && \text{for forced convection} \end{aligned} \tag{3.15}$$

where g gravitational acceleration, $\alpha_{T,flu}$ coefficient of thermal expansion (CTE) of the fluid, $l_{c,Cr}$ characteristic length of the natural convection [m], D_t thermal diffusivity; υ_f fluid kinematic viscosity; $l_{c,Re}$ characteristic length of the forced convective flux, v wind velocity; and λ_{flu} thermal conductivity of the fluid.

Lee et al. (2009) reported convective heat transfer coefficient of concrete exposed to air from 9.0 to 13.0 W/(m^2K) for wind velocities ranging from 2.0 to 3.0 m/s.

When concrete surface is covered with layers of other materials (arranged in series), such as formwork, insulation sheets or ground, the heat transfer coefficient due to the additional layers is expressed as follows:

$$\sum_{i=1}^{n}\frac{1}{h_i} = \frac{t_1}{\lambda_1} + \frac{t_2}{\lambda_2} + \cdots + \frac{t_i}{\lambda_i} \tag{3.16}$$

where h_i is the heat exchange coefficient of each layer, with t_i as the thickness of a layer, and λ_i is the corresponding thermal conductivity. A list of thermal conductivities of commonly used insulating materials can be found, e.g., in Jonasson (1994).

For the cases in which the boundary element is thick, or the concrete is merely in contact with soil, an older foundation or adjacent elements, significant heat can be accumulated in such an adjoining element. Therefore, the assumption at the basis of Eq. 3.16 ceases to be valid and such boundary or adjacent elements need to be explicitly considered in the models. When the adjacent member has well-determined geometry/size (e.g. a thick formwork with insulation panel), it can be modelled in full. When such element is geometrically indeterminate, such as a foundation terrain, it is necessary to introduce simplifications. Normally, the underlying terrain may be modelled to such an extent that temperature variations due to the environmental changes and the self-heating concrete cannot significantly affect the initial temperature of the most distant points of the underlying terrain included in the model (Azenha 2009).

A further heat exchange mechanism, in addition to convection or radiation at the surface, takes place on wet surfaces of fresh concrete exposed to evaporation, in particular horizontal concrete surfaces covered with bleeding water (which may accumulate on the top of fresh concrete) or covered with curing water (Hasanain et al. 1989). The phase change due to evaporation of water and the associated consumption of energy (heat of evaporation) together lead to evaporative cooling of concrete surfaces. By using a combination of experiments and simulations, Azenha et al. (2007a, b) have demonstrated the importance of evaporative cooling in hot and dry environments, which enforced near-surface temperature drops of up to 7 °C when insulation was removed from previously sealed cement paste specimens (temperature of 36 °C and relative humidity of 30%). They have further shown that this effect is strongly diminished and becomes almost negligible when non-extreme environments are considered, e.g. temperature of 20 °C and relative humidity of 60%.

A rapid decrease of the surface temperature, as opposed to the self-heating bulk, may lead to the formation of high temperature gradient and cracking (Kovler 1995). To avoid this effect, limiting of early-age evaporation can be applied by means of covering the surface with, e.g., plastic sheets (McCarter and Ben-Saleh 2001). On the other hand, this effect was reported to be only very limited in time in the situations where bleeding water evaporates fast, especially with high ambient temperature and high wind speed (Hasanain et al. 1989).

To estimate the effect of heat exchange due to evaporative cooling, the mass exchange with the environment needs to be considered explicitly. In Azenha et al. (2007a), several numerical simulations with the DuCOM simulation framework were performed, and the near-surface temperature variations associated with evaporative cooling could be predicted by combining a hygrothermal analysis with a simple coupling term regarding the enthalpy of water evaporation.

3.2 Coefficient of Thermal Expansion (CTE)

In order to quantify the vulnerability of concrete to the restrained thermal deformations and therefore to the cracking risk, a coefficient expressing the tendency of concrete to deform due to temperature changes is used. Even though the term *coefficient of thermal expansion* (CTE) formally refers to the volume or length increase (expansion) upon heating only, it is often used in the literature to describe volume/length changes acting in both directions, due to both heating and cooling. The more general term *coefficient of thermal dilation* (CTD) is sometimes used and is formally more appropriate. Here, similarly as in most of the literature, the term CTE will be used to describe deformations in either direction and therefore will be considered as the equivalent of CTD. The CTE described thereafter, unless otherwise specified, refers to the linear coefficient expressing length change (contraction or expansion) at unit change of temperature (cooling or heating, respectively) (ARMY-COE 1981).

Different methods exist for the determination of the CTE based on the same principle: determining deformations and relating the deformation to the known temperature history, either applied as a part of a test, or self-induced by the hydrating material (Boulay 2003). The methods can be in general divided into linear and volumetric. It is normally assumed that the volumetric thermal expansion is isotropic; thus, the linear CTE can be approximated as one-third of the volumetric one. In the linear method, elongation and shortening of a sample exposed to changing temperature are followed by either measurements of the sample length change with, e.g., LVDTs or optical systems or by strain measurements on the sample with, e.g., length comparators, strain gauges or vibrating wire extensometer, e.g. Kada et al. (2002); Buch and Jahangirnejad (2008); Maruyama and Teramoto (2011); ASTM (2012); AASHTO (2011); Azenha and Granja (2015). Linear techniques are often applied for in situ measurements of the CTE in the field, e.g. Yeon et al. (2013).

In the volumetric method, the sample is immersed in a bath containing a liquid of known density, see, e.g., Loser et al. (2010). By suspending the sample from a scale, the volume changes can be followed by measuring the apparent mass changes of the immersed sample. A systematic study of different factors influencing the volumetric method has been presented in Loser et al. (2010), where it was also shown that linear and volumetric methods give comparable results when all main artefacts are eliminated with care.

When thermal deformations are measured at early ages, they are often (especially for concretes with lower w/c) occurring simultaneously with autogenous shrinkage. Therefore, assuming the validity of the superposition principle, autogenous shrinkage needs to be subtracted from the total deformation to separate the thermal component (Bjøntegaard and Sellevold 2001; Loser et al. 2010; Wyrzykowski and Lura 2013a; Cusson and Hoogeveen 2007). Such assumption of superposition of thermal and autogenous components is valid when small temperature changes are considered (i.e. up to couple degrees) and the temperature steps are short (i.e. up to about 1–2 h) considering the ongoing hydration process. For larger temperature changes lasting longer, the dependence of the autogenous shrinkage upon temperature needs to be taken into account as well (Jensen and Hansen 1999; Bjøntegaard and Sellevold 2001; Maruyama and Teramoto 2011); in such case, the CTE is subject to possible bias due to an inaccurate estimation of autogenous shrinkage. General recommendations on testing procedures for CTE and autogenous shrinkage prepared based on the round robin test campaign of RILEM TC195-DTD are presented in Hammer and Bjøntegaard (2006).

It has long been observed that the CTE changes considerably during setting and hardening of concrete, e.g. Sellevold and Bjøntegaard (2006); Yeon et al. (2013). Similarly to other thermal properties (i.e. conductivity, heat capacity), since aggregates are inert, the evolution of the CTE is due to hardening and moisture state changes in the cement paste. Sellevold and Bjøntegaard (2006) have shown that hydration has only a negligible net effect on the evolution of the CTE, since concrete rewetted at the age of a couple of weeks had similar CTE as wet concrete shortly after setting time. Numerous studies have shown that the CTE of cement paste (and therefore also of concrete) changes considerably with the moisture state of the material (Kovler and Zhutovsky 2006; Sellevold and Bjøntegaard 2006;Grasley and Lange 2007; Maruyama and Teramoto 2012; Wyrzykowski and Lura 2013a, b). A general trend of the CTE evolution in cement paste is shown in Fig. 3.2.

It can be seen that the very high initial CTE is due to the contribution of water when concrete or cement paste is still in the plastic state. Shortly after setting time, a sudden decrease is observed. The value at this point corresponds to the CTE of the

Fig. 3.2 Evolution of CTE of w/c 0.30 cement paste and mortar (with 40% vol. aggregates) during hardening in sealed conditions. For details, see Wyrzykowski and Lura (2013a)

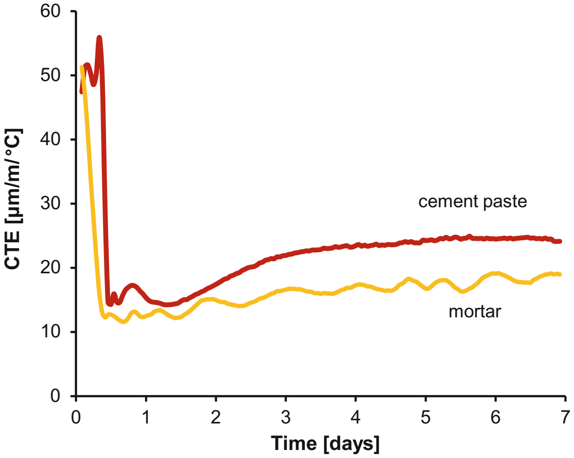

solid skeleton, and, as already mentioned, should not change considerably due to hydration. An increase of the CTE is, however, further observed due to desaturation of the pores in the cement paste. In low *w*/*c* cement paste, an increase of more than 100% respect to the value at setting was observed in (Sellevold and Bjøntegaard 2006; Loser et al. 2010; Wyrzykowski and Lura 2013a, b). The moisture dependence of the CTE has been shown to be due to the temperature dependence of sorption. With increasing temperature, the RH in the pores increases, causing hygral swelling acting in addition to the thermal dilation of the solids. This effect becomes higher at RH decreasing from 100% to approximately 50%, see Sellevold and Bjøntegaard (2006); Radjy et al. (2003). The increase of the CTE is particularly important in low *w*/*c* pastes, in which the internal RH decreases considerably due to self-desiccation. Nevertheless, a considerable increase in CTE was observed in Wyrzykowski and Lura (2013b) for cement pastes with *w*/*c* as high as 0.45. In any case, desaturation of pores of concrete due to external drying will also result in a CTE increase (Sellevold and Bjøntegaard 2006).

Considering that the aggregates commonly used in concrete have lower CTE than the cement paste (see Table 3.3), due to the restraining effect of aggregates, the effect of the desaturation of the cement paste on the overall CTE of concrete is naturally lower than in cement paste or mortar (Sellevold and Bjøntegaard 2006; Wyrzykowski and Lura 2013b; Yeon et al. 2013). However, as reported by Sellevold and Bjøntegaard (2006), an increase from about 7 µm/m/°C at the time of setting to about 11 µm/m/°C after drying was observed in concrete with 72% vol. of aggregates. Furthermore, experimental results starting at the initial set are reported in Delsaute and Staquet (2017). It was found that the CTE increases from a minimum value varying between 7 and 9 µm/m/°C to a value varying between 10 and 12 µm/m/°C for concretes with w/c ranging from 0.4 to 0.6 during the hydration process, when the concrete is kept in sealed condition. Also, as shown by

Table 3.3 CTE of concrete and different types of aggregates as reported in the literature. Whenever the evolution of the CTE was followed, values after setting are reported here

Material/condition	CTE [µm/m/°C]	References
Concrete w/c 0.40, 72% vol. aggregates, 5% silica fume	7–11 (100–88% saturation degree)	Sellevold and Bjøntegaard (2006)
Concrete w/c 0.45, ~74% vol. aggregates, limestone coarse aggregate	5–7	Yeon et al. (2013)
Concrete w/c 0.45, ~71% vol. aggregates, river gravel coarse aggregate	8–9	Yeon et al. (2013)
Concretes w/c 0.30–0.45, ~66% vol. aggregates, metamorphic limestone-based coarse aggregate	6.5–7.6	Kada et al. (2002)
Concretes: normal (w/c 0.45) and high strength (w/c 0.25 and w/c 0.31), ~70% vol. aggregates (limestone)	10–11	Cook et al. (1993)
Concrete (recommendation)	11	ACI (2001)
Concrete, ~70% vol. aggregates, gravel coarse aggregate (6 different sources), w/b 0.40 (saturated, 28 d)	9.7–10.7	Naik et al. (2010)
Concrete, ~67% vol. aggregates, basalt coarse aggregate, w/b 0.40 (saturated, 28 d)	9.3	Naik et al. (2010)
Concrete (typical value)	10–12	Bentz (2008)
Aggregate: granite	7–9	Mindess et al. (2003)
Aggregate: basalt	6–8	Mindess et al. (2003)
Aggregate: limestone	6	Mindess et al. (2003)
Aggregate: dolomite	7–10	Mindess et al. (2003)
Aggregate: sandstone	11–12	Mindess et al. (2003)
Aggregate: quartzite	11–13	Mindess et al. (2003)

the numerical study by Yeon et al. (2013), the evolution of CTE due to desaturation in concrete can considerably affect the early-age thermal stresses.

As an efficient way for reducing the increase of CTE during hardening, internal curing has been proposed. It has been shown that the CTE can be reduced to values occurring shortly after setting, both using lightweight aggregates (Maruyama and Teramoto 2012) and superabsorbent polymers (Wyrzykowski and Lura 2013b).

It has been observed that, above the freezing point of water in the pores, the CTE increases slightly with temperature (Kodur 2014). However, for the temperature range normally encountered in massive structures, this effect is usually neglected (Briffaut et al. 2012; de Schutter 2002; Faria et al. 2006; Liu et al. 2014; Yuan and Wan 2002; Zreiki et al. 2010; ACI 2001).

The coefficient of thermal expansion of concrete varies strongly with concrete mix constituents (particularly aggregate type and amount) (CEB-FIP 2013;

Bangash 2001). A comprehensive study on the effect of different aggregates can be found in Buch and Jahangirnejad (2008). Some CTE values for concrete, either measured directly or assumed in calculations, are reported in Table 3.3.

As shown by Wyrzykowski and Lura (2013b), the dependence of the CTE upon the mix composition can be estimated with a good accuracy based on effective medium approaches, e.g. the Hobbs model (Hobbs 1971) or the Rosen–Hashin bounds (Rosen and Hashin 1970), when the CTE of the mix constituents is known, see Table 3.3. Zhutovsky and Kovler (2017) proposed a poromechanical model for the estimation of the CTE of concrete using the evolution of elastic properties obtained from ultrasonic measurements as input.

References

AASHTO. (2011). T 336 Standard method of test for coefficient of thermal expansion of hydraulic cement concrete. Washington, D.C.: American Association of State Highway and Transportation Officials.

Abdolhosseini Qomi, M. J., Ulm, F.-J., & Pellenq, R. J.-M. (2015). Physical origins of thermal properties of cement paste. *Physical Review Applied, 3,* 064010.

ACI. (2001). ACI 224.3R-95: Joints in concrete construction. Farmington Hills, MI.

ACI. (2005). ACI 207.1R-05: Guide to mass concrete. Farmington Hills, MI.

ARMY-COE CRD-C 39-81. (1981). *Handbook for Concrete and Cement Test Method for Coefficient of Linear Thermal Expansion of Concrete*.

ASTM C531-00. (2012). *Standard test method for linear shrinkage and coefficient of thermal expansion of chemical-resistant mortars, grouts, monolithic surfacings, and polymer concretes*. West Conshohocken, PA: ASTM International.

ASTM C1113/C1113M-09. (2013). *Standard test method for thermal conductivity of refractories by hot wire (Platinum resistance thermometer technique)*. West Conshohocken, PA: ASTM International.

Azenha, M., Maekawa, K., Ishida, T., & Faria, R. (2007a). Drying induced moisture losses from mortar to the environment. Part I: Experimental research. *Materials and Structures, 40,* 80–811.

Azenha, M., Maekawa, K., Ishida, T., & Faria, R. (2007b). Drying induced moisture losses from mortar to the environment. Part II: Numerical implementation. *Materials and Structures, 40,* 813–825.

Azenha, M. (2009). Numerical simulation of the structural behaviour of concrete since its early ages. Ph.D. thesis, Faculty of Engineering of the University of Porto, Portugal.

Azenha, M., Sousa, C., Faria, R., & Neves, A. (2011). Thermo–hygro–mechanical modelling of self-induced stresses during the service life of RC structures. *Engineering Structures, 33,* 3442–3453.

Azenha, M, & Granja, J. (2015). Characterization of concrete properties at early ages: Case studies of the University of Minho. *CMS Workshop "Cracking of Massive Concrete Structures", eBook of Presentations (RILEM)*, March 17, 2015. ENS-Cachan, Paris.

Bangash, M. Y. H. (2001). *Manual of numerical methods in concrete*. London, UK: Thomas Telford Ltd.

Baquerizo, L. G., Matschei, T., Scrivener, K. L., et al. (2015). Hydration states of AFm cement phases. *Cement and Concrete Research, 73,* 143–157.

Bentz, D. (2007). Transient plane source measurements of the thermal properties of hydrating cement pastes. *Materials and Structures, 40,* 1073–1080.

Bentz, D. (2008). A review of early-age properties of cement-based materials. *Cement and Concrete Research, 38*(2), 196–204.

Bentz, D., Peltz, M., Duran-Herrera, A., Valdez, P., & Juarez, C. (2011). Thermal properties of high-volume fly ash mortars and concretes. *Journal of Building Physics, 34*(3), 263–275.

Bentz, D. P., & Prasad, K. R. (2007). Thermal performance of fire resistive materials. I. Characterization with respect to thermal performance models. NISTIR 7401, National Institute of Standards and Technology, Gaithersburg, MD, USA.

Bjøntegaard, Ø., & Sellevold, E. J. (2001). Interaction between thermal dilation and autogenous deformation in high performance concrete. *Materials and Structures, 34,* 266–272.

Bohm, H. J., & Nogales, S. (2008). Mori-Tanaka models for the thermal conductivity of composites with interfacial resistance and particle size distributions. *Composites Science and Technology, 68*(5), 1181–1187.

de Borst, R., & van den Boogaard, A. H. (1994). Finite-element modeling of deformation and cracking in early-age concrete. *ASCE Journal of the Engineering Mechanics, 120*(12), 2519–2534.

Boulay, C. (2003). Determination of the coefficient of thermal expansion. Early age cracking in cementitious systems. Report of RILEM Technical Committee 181-EAS—Early age shrinkage induced stresses and cracking in cementitious systems (pp. 217–224). RILEM Publications SARL.

Branco, F. A., Mendes, P. A., & Mirambell, E. (1992). Heat of hydration effects in concrete structures. *ACI Materials Journal, 89*(2), 139–145.

van Breugel, K. (1980). *Artificial cooling of hardening concrete*. Delft University of Technology. Concrete Structures, Delft.

Briffaut, M., Benboudjema, F., Torrenti, J. M., & Nahas, G. (2012). Effects of the early age thermal behaviour on long term damage risk in massive concrete structures. *European Journal of Environmental and Civil Engineering, 16*(5), 598–605.

Buch, N. J., & Jahangirnejad, S. (2008). Quantifying coefficient of thermal expansion values of typical hydraulic cement concrete paving mixtures (No. RC-1503). Michigan Department of Transportation, Construction & Technology Division.

Campbell-Allen, D., & Thorne, C. P. (1963). The thermal conductivity of concrete. *Magazine of Concrete Research, 15*(43), 39–48.

CEB-FIP *fib*. (2013). Bulletin 70. State-of-the-art report: Code-type models for concrete behaviour. Background of MC2010.

Cerny, R., & Rovnanikova, P. (2002). *Transport processes in concrete*. CRC Press.

Choktaweekarn, P., & Tangtermsirikul, S. (2010). Effect of aggregate type, casting, thickness and curing condition on restrained strain of mass concrete. *Songklanakarin Journal of Science and Technology, 32,* 391–402.

Cook, W. D., Aitcin, P. C., & Mitchell, D. (1993). Thermal stresses in large high-strength concrete columns. *ACI Materials Journal, 89*(1), 61–68.

Côté, J., & Konrad, J.-M. (2005). A generalized thermal conductivity model for soils and construction materials. *Canadian Geotechnical Journal, 42,* 443–458.

Coussy, O. (2005). *Poromechanics*. Chichester: Wiley.

Craeye, B., de Schutter, G., Humbeeck, H. V., & Cotthem, A. V. (2009). Early age behaviour of concrete supercontainers for radioactive waste disposal. *Nuclear Engineering and Design, 239*, 23–35.

Cusson, D., & Hoogeveen, T. (2007). An experimental approach for the analysis of early-age behaviour of high-performance concrete structures under restrained shrinkage. *Cement and Concrete Research, 37,* 200–209.

Delsaute, B., & Staquet, S. (2017). Decoupling thermal and autogenous strain of concretes with different water/cement ratios during the hardening process. *Advances in Civil Engineering Materials, 6*(2), 1–22.

Faria, R., Azenha, M., & Figueiras, J. A. (2006). Modelling of concrete at early ages: Application to an externally restrained slab. *Cement and Concrete Research, 28,* 572–585.

Gawin, D., Majorana, C. E., & Schrefler, B. A. (1999). Numerical analysis of hygro-thermic behaviour and damage of concrete at high temperature. *Mechanics of Cohesive-Frictional Materials, 4,* 37–74.

Gawin, D., Pesavento, F., & Schrefler, B. A. (2006). Hygro-thermo-chemo-mechanical modelling of concrete at early ages and beyond. Part I: Hydration and hygro-thermal phenomena. *International Journal for Numerical Methods in Engineering, 67,* 299–331.

Gibbon, G. J., & Ballim, Y. (1998). Determination of the thermal conductivity of concrete during the early stages of hydration. *Magazine of Concrete Research, 50,* 229–235.

Guo, L., Guo, L., Zhong, L., & Zhu, Y. (2011). Thermal conductivity and heat transfer coefficient of concrete. *Journal of Wuhan University of Technology-Materials Science Edition, 26*(4), 791–796.

Grasley, Z., & Lange, D. (2007). Thermal dilation and internal relative humidity of hardened cement paste. *Materials and Structures, 40*(3), 311–317.

Hammer, T. A., & Bjøntegaard, Ø. (2006). Testing of autogenous deformation (AD) and thermal dilation (TD) of early age mortar and concrete—Recommended test procedure. In *International RILEM Conference on Volume Changes of Hardening Concrete: Testing and Mitigation* (pp. 341–346). RILEM Publications SARL.

Hammerschmidt, U. (2002). Guarded hot-plate (GHP) method: Uncertainty assessment. *International Journal of Thermophysics, 23*(6), 1551–1570.

Hamzah, M. O., Jamshidi, A., & Shahadan, Z. (2010). Evaluation of the potential of sasobit to reduce required heat energy and co2 emission in the asphalt industry. *Journal of Cleaner Production, 18*(18), 1859–1865.

Hasanain, G. S., Khallaf, T. A., & Mahmood, K. (1989). Water evaporation from freshly placed concrete surfaces in hot weather. *Cement and Concrete Research, 19*(3), 465–475.

Hobbs, D. (1971). The dependence of the bulk modulus, Young's modulus, creep, shrinkage and thermal expansion of concrete upon aggregate volume concentration. *Materials and Structures, 4*(2), 107–114.

Hollick, J. (2012). Nocturnal radiation cooling tests. *Energy Procedia, 30,* 930–936.

Holman, J. (2009). *Heat transfer* (10th ed.). Boston: McGraw-Hill Education.

Honorio, T. (2015). Modelling concrete behaviour at early-age: Multiscale analysis and simulation of a massive disposal structure. Ph.D. thesis, ENS Cachan, Univeristé Paris-Saclay.

Honorio, T., Bary, B., & Benboudjema, F. (2018). Thermal properties of cement-based materials: Multiscale estimations at early-age. *Cement and Concrete Composites, 87*, 205–219.

Jendele, L., Šmilauer, V., & Cervenka, J. (2014). Multiscale hydro–thermo–mechanical model for early-age and mature concrete structures. *Advances in Engineering Software, 72*, 134–146.

Jensen, O. M., & Hansen, P. F. (1999). Influence of temperature on autogenous deformation and relative humidity change in hardening cement paste. *Cement and Concrete Research, 29,* 567–575.

Jonasson, J.-E. (1994). Modelling of temperature, moisture and stress in young concrete. Ph.D. thesis, Luleå University of Technology, Luleå, Sweden.

Kada, H., Lachemi, M., Petrov, N., Bonneau, O., & Aitcin, P. C. (2002). Determination of the coefficient of thermal expansion of high performance concrete from initial setting. *Materials and Structures, 35,* 35–41.

Khan, M. I. (2002). Factors affecting the thermal properties of concrete and applicability of its prediction models. *Building and Environment, 37,* 607–614.

Kim, K. H., Jeon, S. E., Kim, J. K., & Yang, S. (2003). An experimental study on thermal conductivity of concrete. *Cement and Concrete Research, 33*(3), 363–371.

Klemczak, B. (2011). Prediction of coupled heat and moisture transfer in early-age massive concrete structures. *Numerical Heat Transfer, Part A: Applications, 60,* 212–233.

Kodur, V. (2014). Properties of Concrete at Elevated Temperatures. *ISRN Civil Engineering, 2014,* 468510.

Kovler, K. (1995). Shock of evaporative cooling of concrete in hot dry climate. *Concrete International, 17*(10), 65–69.

Kovler, K., & Zhutovsky, S. (2006). Overview and future trends of shrinkage research. *Materials and Structures, 39*(9), 827–847.

Kusuda, T. (1977). Fundamentals of building heat transfer. *Journal of Research of the National Bureau of Standards, 82*(2).

Kwak, H.-G., Ha, S.-J., & Kim, J.-K. (2006). Non-structural cracking in RC walls. Part I: Finite element formulation. *Cement and Concrete Research, 36*, 749–760.

Lee, Y., Choi, M. S., Yi, S. T., & Kim, J. K. (2009). Experimental study on the convective heat transfer coefficient of early-age concrete. *Cement and Concrete Composites, 31*(1), 60–71.

Litovsky, E. Y., & Shapiro, M. (1992). Gas pressure and temperature dependences of thermal conductivity of porous ceramic materials: Part 1, Refractories and ceramics with porosity below 30%. *Journal of American Ceramic Society, 75,* 3425–3439.

Liu, X., Jiang, W., de Schutter, G., Yuan, Y., & Su, Q. (2014). Early-age behaviour of precast concrete immersed tunnel based on degree of hydration concept. *Structural Concrete, 15*(1), 66–80.

Loser, R., Münch, B., & Lura, P. (2010). A volumetric technique for measuring the coefficient of thermal expansion of hardening cement paste and mortar. *Cement and Concrete Research, 40* (7), 1138–1147.

Lothenbach, B., Matschei, T., Möschner, G., & Glasser, F. P. (2008). Thermodynamic modelling of the effect of temperature on the hydration and porosity of Portland cement. *Cement and Concrete Research, 38,* 1–18.

Luca, J., & Mrawira, D. (2005). New measurement of thermal properties of superpave asphalt concrete. *Journal of Materials in Civil Engineering, 17*(1), 72–79.

Lura, P., & Van Breugel, K. (2001). Thermal properties of concrete: sensitivity studies. Report: Improved Production of Advanced Concrete (IPACS). Lulea University of Technology.

Marshall, A. L. (1972). The thermal properties of concrete. *Building Science, 7,* 167–174.

Maruyama, I., & Teramoto, A. (2011). Impact of time-dependant thermal expansion coefficient on the early-age volume changes in cement pastes. *Cement and Concrete Research, 41,* 380–391.

Maruyama, I., & Teramoto, A. (2012). Effect of water-retaining lightweight aggregate on the reduction of thermal expansion coefficient in mortar subject to temperature histories. *Cem Concr Compos, 34*(10), 1124–1129.

Matschei, T., Lothenbach, B., & Glasser, F. P. (2007). Thermodynamic properties of Portland cement hydrates in the system $CaO–Al_2O_3–SiO_2–CaSO_4–CaCO_3–H_2O$. *Cement and Concrete Research, 37,* 1379–1410.

McCarter, W. J., & Ben-Saleh, A. M. (2001). Influence of practical curing methods on evaporation of water from freshly placed concrete in hot climates. *Built Environment, 36*(8), 919–924.

Mehta P, Monteiro P (2005) Concrete: Microstructure, Properties, and Materials. McGraw-Hill.

Michell, D., & Biggs, K. L. (1979). Radiation cooling of buildings at night. *Applied Energy, 5*(4), 263–275.

Mindess, S., Young, J. F., & Darwin, D. (2003). *Concrete* (2nd ed.). Upper Saddle River: Prentice-Hall.

Modest, M. F. (2013). *Radiative heat transfer*. Academic press.

Morabito, P. (1989). Measurement of the thermal properties of different concretes. *High Temperatures High Pressures, 21*(1), 51–59.

Mounanga, P., Khelidj, A., & Bastian, G. (2004). Experimental study and modelling approaches for the thermal conductivity evolution of hydrating cement paste. *Advances in Cement Research, 16,* 95–103.

Naik, T. R., Kraus, R. N., & Kumar, R. (2010). Influence of types of coarse aggregates on the coefficient of thermal expansion of concrete. *Journal of Materials in Civil Engineering, 23*(4), 467–472.

Neville, A. M. (1997). *Properties of concrete* (4th ed.). London, UK: Wiley.

Pomianowski, M., Heiselberg, P., Jensen, R. L., Cheng, R., & Zhang, Y. (2014). A new experimental method to determine specific heat capacity of inhomogeneous concrete material with incorporated microencapsulated-PCM. *Cement and Concrete Research, 55,* 22–34.

Radjy, F., Sellevold, E. J., & Hansen, K. K. (2003). Isosteric vapor pressure—Temperature data for water sorption in hardened cement paste: Enthalpy, entropy and sorption isotherms at different temperatures. Report BYG-DTU R-057. Lyngby: Technical University of Denmark.

Reinhardt, H.-W., Blauwendraad, J., & Jongendijk, J. (1982). Temperature development in concrete structures taking account of state dependent properties. In *International Conference on Concrete at Early Ages*, RILEM, Paris (pp. 211–218).

Rosen, B. W., & Hashin, Z. (1970). Effective thermal expansion coefficients and specific heats of composite materials. *International Journal of Engineering Science, 8*(2), 157–173.

de Schutter, G. (2002). Finite element simulation of thermal cracking in massive hardening concrete elements using degree of hydration based material laws. *Computers & Structures, 80,* 2035–2042.

Ruiz, J., Schindler, A., Rasmussen, R., Kim, P., & Chang, G. (2001). Concrete temperature modeling and strength prediction using maturity concepts in the FHWA HIPERPAV software. In *7th International Conference on Concrete Pavements*, Orlando (FL), USA, 2001.

Sellevold, E. J., & Bjøntegaard, Ø. (2006). Coefficient of thermal expansion of cement paste and concrete: Mechanisms of moisture interaction. *Materials and Structures, 39,* 809–815.

Tatro, S. B. (2006). Thermal properties. In J. F. Lamond & J. H. Pielert (Eds.), *Significance of tests and properties of concrete and concrete-making materials, STP169D-EB* (p. 2006). West Conshohocken, PA: ASTM International.

Todd, S. (1951). Low-temperature heat capacities and entropies at 298.16 °K of crystalline calcium orthosilicate, zinc orthosilicate and tricalcium silicate. *Journal of the American Chemical Society, 73,* 3277–3278.

Ulm, F. J., & Coussy, O. (2001). What is a “massive” concrete structure at early ages? Some dimensional arguments. *Journal of Engineering Mechanics, 127,* 512–522.

Vargaftik, N. B. (1993) *Handbook of thermal conductivity of liquids and gases*. CRC Press.

Wojcik, G. S. (2001). The interaction between the atmosphere and curing concrete bridge decks. Ph.D. thesis, State University of New York at Albany, Dissertation Abstracts International (Vol. 63-01, Section: B).

Wojcik, G. S., Fitzjarrald, D. R., & Plawsky, J. L. (2003). Modelling the interaction between the atmosphere and curing concrete bridge decks with the SLABS model. *Meteorological Applications, 10*(2), 165–186.

Wyrzykowski, M., & Lura, P. (2013a). Moisture dependence of thermal expansion in cement-based materials at early ages. *Cement and Concrete Research, 53,* 25–35.

Wyrzykowski, M., & Lura, P. (2013b). Controlling the coefficient of thermal expansion of cementitious materials—A new application for superabsorbent polymers. *Cement and Concrete Composites, 35,* 49–58.

Xu, Y., & Chung, D. D. L. (2000). Effect of sand addition on the specific heat and thermal conductivity of cement. *Cement and Concrete Research, 30,* 59–61.

Yeon, J. H., Choi, S., & Won, M. C. (2013). In situ measurement of coefficient of thermal expansion in hardening concrete and its effect on thermal stress development. *Construction and Building Materials, 38,* 306–315.

Yuan, Y., & Wan, Z. L. (2002). Prediction of cracking within early-age concrete due to thermal, drying and creep behavior. *Cement and Concrete Research, 32,* 1053–1059.

Zreiki, J., Bouchelaghema, F., & Chaouchea, M. (2010). Early-age behaviour of concrete in massive structures—Experimentation and modelling. *Nuclear Engineering and Design, 240,* 2643–2654.

Zhutovsky, S., & Kovler, K. (2017). Application of ultrasonic pulse velocity for assessment of thermal expansion coefficient of concrete at early age. *Materials and Structures, 50*(5), 8.